Earth and Planetary Science Letters xxx (2009) xxx–xxx

Contents lists available at ScienceDirect

Earth and Planetary Science Letters

journal homepage: www.elsevier.com/locate/epsl

Late Pleistocene California droughts during deglaciation and Arctic warming

Jessica L. Oster [a,*], Isabel P. Montañez [a], Warren D. Sharp [b], Kari M. Cooper [a]

[a] Geology Department, University of California, Davis, California, United States
[b] Berkeley Geochronology Center, Berkeley, California, United States

ARTICLE INFO

Article history:
Received 4 February 2009
Received in revised form 4 August 2009
Accepted 7 October 2009
Available online xxxx

Editor: P. DeMenocal

Keywords:
speleothem
Sierra Nevada paleoclimate
deglacial
stable and radiogenic isotopes
trace elements
U-series

ABSTRACT

Recent studies document the synchronous nature of shifts in North Atlantic regional climate, the intensity of the East Asian monsoon, and productivity and precipitation in the Cariaco Basin during the last glacial and deglacial period. Yet questions remain as to what climate mechanisms influenced continental regions far removed from the North Atlantic and beyond the direct influence of the inter-tropical convergence zone. Here, we present U-series calibrated stable isotopic and trace element time series for a speleothem from Moaning Cave on the western slope of the central Sierra Nevada, California that documents changes in precipitation that are approximately coeval with Greenland temperature changes for the period 16.5 to 8.8 ka.

From 16.5 to 10.6 ka, the Moaning Cave stalagmite proxies record drier and possibly warmer conditions, signified by elevated $\delta^{18}O$, $\delta^{13}C$, [Mg], [Sr], and [Ba] and more radiogenic $^{87}Sr/^{86}Sr$, during Northern Hemisphere warm periods (Bølling, early and late Allerød) and wetter and possibly colder conditions during Northern Hemisphere cool periods (Older Dryas, Inter-Allerød Cold Period, and Younger Dryas). Moaning Cave stable isotope records indicate that wet conditions persisted in this area well beyond 11.5 ka, suggesting the effects of the Younger Dryas event may have been longer lived in the western Sierra Nevada than in Greenland. However, a shifting drip center and corresponding change in seepage water routing may have influenced the trace element records between 10.6 and 9.6 ka. Linkages between northern high-latitude climate and precipitation in the Sierra Nevada suggested here could indicate that, under conditions of continued global warming, this drought-prone region may experience a reduction in Pacific-sourced moisture.

1. Introduction

Abrupt changes in temperature of up to 20 °C over Greenland that persisted for centuries to millennia during the last glacial and ensuing deglacial periods (Alley et al., 1993; Stuiver and Grootes, 2000) coincided with widespread perturbation of North Atlantic regional climate (Labeyrie, 2000; Bond et al., 2001; Broecker, 2003; Hemming, 2004; Kienast et al., 2006). Recent studies document the interhemispheric nature of these climate events with coincident changes in the intensity of the southeast Asian monsoon, surface water temperature in the Santa Barbara Basin (eastern Pacific), productivity and precipitation in the Cariaco Basin (Caribbean), and continental climates throughout the Northern and Southern Hemisphere tropics and subtropics (e.g., Peterson et al., 2000; Wang et al., 2001; Hendy et al., 2002; Lea et al., 2003; Yuan et al., 2004; Polyak et al., 2004; Wang et al., 2004, 2005; Denniston et al., 2007). Although model simulations indicate that such widespread, abrupt climate shifts likely occurred via atmospheric teleconnections between these areas and the northern high-latitudes (Manabe and Stouffer, 1988; Mikolajewicz et al., 1997; Vellinga and Wood, 2002), questions remain as to what climate mechanisms influenced continental regions far removed from the North Atlantic (e.g. western North America) and beyond the direct influence of the inter-tropical convergence zone (ITCZ). Speleothem-bearing caves in the western slope of the Sierra Nevada in California (Fig. 1) offer an opportunity to evaluate the hydroclimate response in western North America to northern high-latitude climate shifts.

The Sierra Nevada are sensitive to changes in atmospheric circulation over the North Pacific given that they are the first major orographic barrier to winter storms brought eastward from the Pacific by the polar jet stream. Model simulations highlight the sensitivity of the average latitude of the polar jet stream and winter storm tracks over western North America to changes in the extent of late Pleistocene North American continental ice sheets (Kutzbach and Wright, 1985; Bromwich et al., 2004, 2005; Kim et al., 2008, Fig. 1), and, more recently, to the extent of Arctic sea ice cover (Sewall and Sloan, 2004; Sewall, 2005) and global warming (Allen and Ingram, 2002; Seager et al., 2007). Stalagmites from caves developed in marble terranes on the western slope of the central Sierra in particular have the potential to provide proxy records of past motions of the polar jet stream and associated precipitation changes (Fig. 1) given their latitudinal position (38 to

* Corresponding author.
E-mail address: joster@ucdavis.edu (J.L. Oster).

0012-821X/$ – see front matter © 2009 Elsevier B.V. All rights reserved.
doi:10.1016/j.epsl.2009.10.003

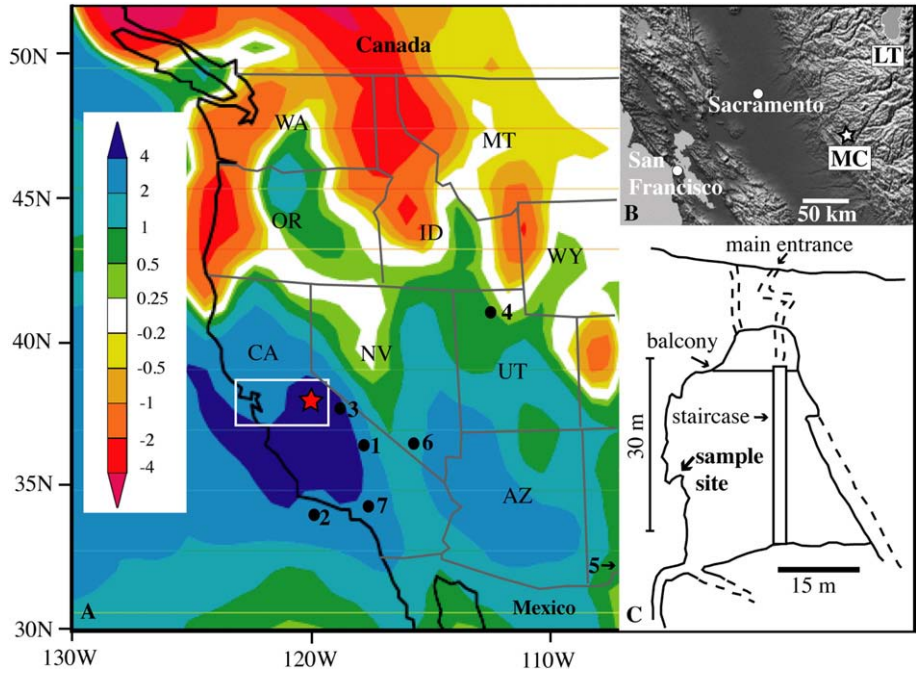

Fig. 1. A) Map of winter precipitation changes from LGM to modern in mm/day from GCM simulation (Kim et al., 2008) shown with location of Moaning Cave (star) and locations of other paleoclimate records mentioned in the text. 1. Owens Lake (e.g. Benson et al., 1996), 2. Santa Barbara Basin (Hendy et al., 2002); 3. Sierra Nevada crest lakes (MacDonald et al., 2008); 4. Great Salt Lake (Oviatt et al., 2005); 5. Guadalupe Mountains caves (Polyak et al., 2004); 6. Devils Hole (Winograd et al., 2006); 7. San Bernardino Mountains, (Owen et al., 2003). B). Relief map of east–west transect across north Central Valley Region, California. MC = Moaning Cave, LT = Lake Tahoe. C) Cross-section through a portion of Moaning Cave showing location of sample collection (after Short, 1975).

39°N) centered between the southernmost extent of the polar jet stream during the Last Glacial Maximum (<37°N) and its present mean winter position (~40°N).

Here, we present isotopic and trace element time series for a speleothem dated by U-series from Moaning Cave, California (Fig. 1). These proxies reveal repeated millennial- to sub-century climate shifts throughout much of the last deglacial period. Stable isotope fluctuations recorded at Moaning Cave share many features that appear coincident — at the resolution of our dating — with interhemispheric-scale climate changes revealed by Greenland ice cores, northern and southern European speleothem and lacustrine records, southeast Asian and Brazilian speleothems, and eastern Pacific and Caribbean marine sediments (Stuiver and Grootes, 2000; Genty et al., 2006; Wang et al., 2001, 2004; Peterson et al., 2000). Abrupt changes in speleothem geochemical proxies at Moaning Cave are interpreted as sudden, marked increases in effective moisture during past cool periods and shifts to significantly drier conditions during past global warmings. At ~12.1 ka there is a shift in the geochemical records from a dominantly climatic signature to one modified by local hydrologic changes. Stable isotopes, however, suggest that wet conditions in the Sierra Nevada foothills beginning at ~12.4 ka, coincident within dating errors with the onset of the Younger Dryas cold period, may have lasted into the early Holocene.

2. Cave geology and setting

Moaning Cave is a vertical solution cavity and dome pit developed along fractures within one of several discrete metamorphosed limestone and dolomite pods of the Calaveras Complex, of the Sierra Nevada foothills (Clark and Lydon, 1962; Bowen, 1973; Short, 1975). The cave has two natural entrances at 520 m above sea level situated above the largest room, which is >37 m tall. Additional rooms extend 64 m below the main room (Short, 1975). An average yearly rainfall of ~430 mm was recorded at Jamestown, California, 13 km to the southeast of Moaning Cave (550 m elevation), between March 2006 and July 2009. Approximately 88% of yearly precipitation falls between October and April when the polar jet stream migrates southward bringing cyclones from the North Pacific into the region. A similar yearly distribution of rainfall (76% during the winter months) occurs at Railroad Flat, a site 26 km to the north of Moaning Cave with longer-duration monitoring (1989–present). Annual rainfall at this site (800 m), however, is higher (820 mm/year).

Natural drip-water flow within the cave increases substantially during the winter season (up to 60 drips per minute) and almost entirely ceases (1 to 2 drips per minute) during the summer. With the exception of the first large rain event of the season, which takes a few days to infiltrate through the epikarst, storm events trigger an almost instantaneous increase in drip-water flow rate within the cave. During the dry summer months, the tourist operation within Moaning Cave pumps water from the aquifer below the cave back through the cave to mimic natural drip water.

Temperature and humidity range from 15.2° to 17.5 °C and 90 to 100%, respectively throughout the year at the sample site within Moaning Cave. Present vegetation above the cave consists of C_3 plants, including manzanita (*Arctostaphylos* sp.), toyon (*Heteromeles arbutifolia*), and other chaparral species. A theoretical equilibrium fractionation temperature (15.6 °C, using Kim and O'Neil, 1997) calculated from the average measured $\delta^{18}O$ value of modern winter drip water (−8.4‰) and the topmost stalagmite calcite (−8.8‰) is close to the measured average winter cave air temperature (16.2 °C), arguing for oxygen isotopic equilibrium in the present MC cave system. Although the top of the stalagmite was wet during collection (collection occurred during the summer), it has not been dated. Additionally, due to the artificial pumping of water into the cave during the summer months, a direct comparison of natural summer drip water to the topmost stalagmite calcite cannot be made for this cave.

3. Methods

3.1. Sample collection

A 2.5 cm diameter core (MC3-A) was drilled through the modern drip center of stalagmite MC3, a meter-wide stalagmite with a rounded

Please cite this article as: Oster, J.L., et al., Late Pleistocene California droughts during deglaciation and Arctic warming, Earth Planet. Sci. Lett. (2009), doi:10.1016/j.epsl.2009.10.003

top that grew 30 m vertically below the cave entrance, using a hand-held electric drill modified by Pomeroy Industries to fit a 30.5 cm long diamond coring bit. At the sample location, the rock thickness above the cave is ~15 m. Although the stalagmite was collected during the dry summer season, the top was wet, and the location of the single drip center was obvious. The stalagmite, which sits on a slope and is ~1.5 m tall along the central axis, is fed by a fracture in the cave ceiling. Four additional cores (MC3-B–MC3-E) (Fig. 2) were drilled around the first core to capture movement of the drip center through time. Core samples, rather than the entire stalagmite, were taken in the interest of cave preservation. Thick (~200 μm) sections were made continuously throughout the top 7 cm of MC3-A where banding is horizontal. Thick sections were also made of the top portions of MC3-B and C (Fig. 2) which each displays sub-horizontal to horizontal banding.

3.2. U-series dating

Four samples for U–Th dating were drilled from MC3-A following visible growth bands. Four additional samples were sawed from MC3-B and C. The locations of samples from these cores were correlated to

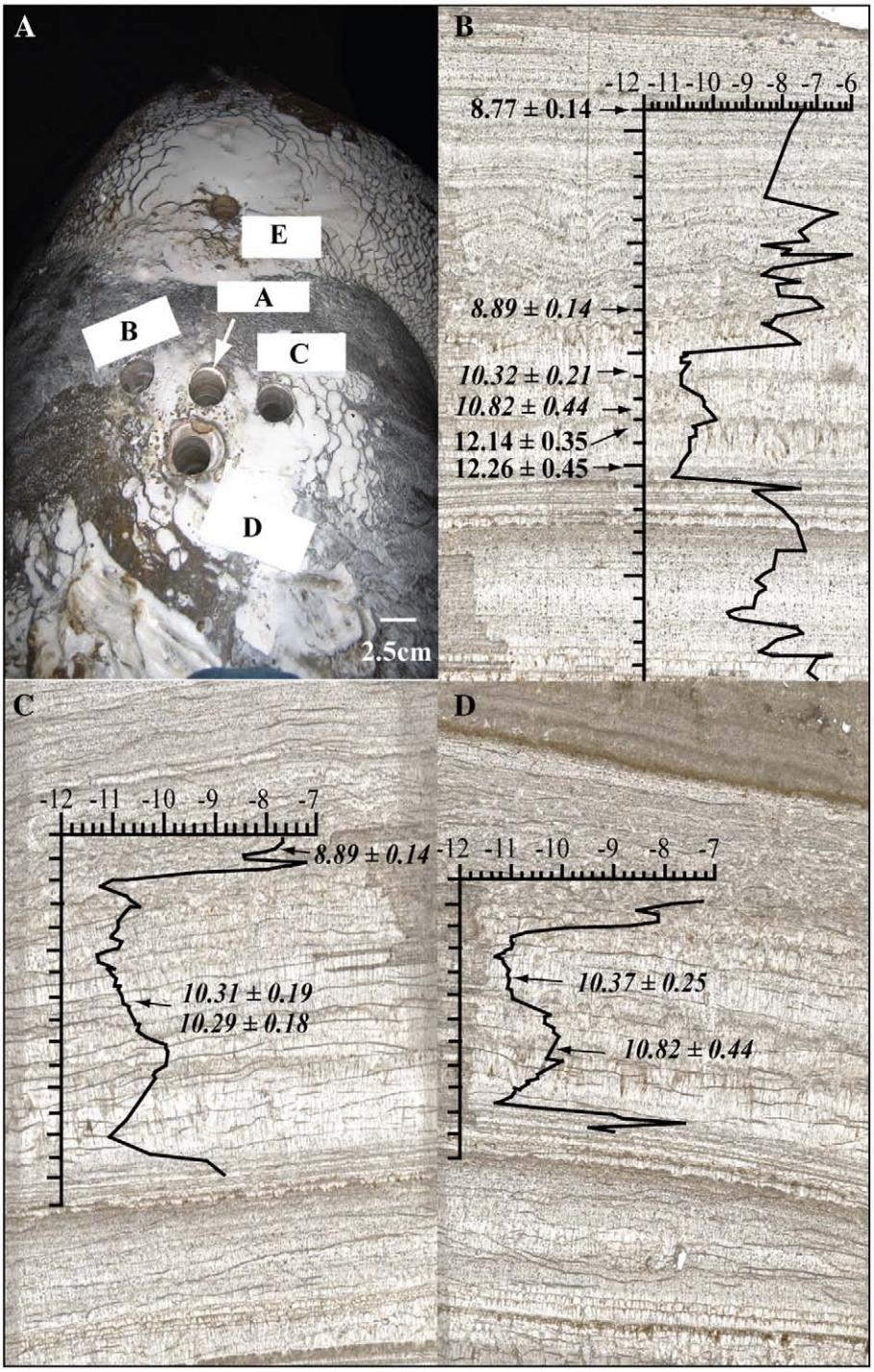

Fig. 2. Comparison of Moaning Cave cores. A) Photograph of sampled stalagmite with core samples MCA-E shown. B) Slide scan image of core MC3-A with $\delta^{13}C$ profile and locations (laminae) of samples for dating indicated by arrows. Dates in italics are taken from cores MC3-B and C. C) Core MC3-B with $\delta^{13}C$profile and dating samples. D) Core MC3-C with $\delta^{13}C$ profile and dating samples. All profiles are given in mm. Note laminae in MC3-B (C) are overprinted by sub-horizontal fractures that occurred during sample preparation.

Please cite this article as: Oster, J.L., et al., Late Pleistocene California droughts during deglaciation and Arctic warming, Earth Planet. Sci. Lett. (2009), doi:10.1016/j.epsl.2009.10.003

MC3-A by visually matching growth bands and $\delta^{18}O$ and $\delta^{13}C$ series among the cores (Fig. 2).

U-series analytical methods are as follows. Samples were dissolved completely in HNO_3–HF–$HClO_4$ and equilibrated with a mixed spike containing ^{229}Th, ^{233}U, and ^{236}U. U and Th were separated using Fe-hydroxide precipitation, followed by two stages of HNO_3–HCl anion exchange chemistry. Th fractions were reacted with $HClO_4$ to remove any residual organic material from ion exchange resins. Purified U and Th fractions were loaded with colloidal graphite onto separate, outgassed rhenium filaments (Edwards et al., 1987). Isotopic analyses were done on a Micromass Sector-54 TIMS equipped with a wide-angle, retarding-potential energy filter and Daly-type ion counter. Mass discrimination for U was corrected using the known $^{233}U/^{236}U$ ratio of the spike, whereas thorium ratios were uncorrected. The U–Th spike was calibrated against solutions of HU-1 (Harwell uraninite) standard and solutions of 69 Ma uranium ore from the Schwartzwalder Mine that have been demonstrated to yield concordant U/Pb ages (Ludwig et al., 1985) and sample-to-sample agreement of $^{234}U/^{238}U$ and $^{230}Th/^{238}U$ ratios. Instrumental performance was monitored by frequent analyses of the Schwartzwalder Mine secular equilibrium standard. Procedural backgrounds for $m/e = 230$ averaged <0.6 fg ^{230}Th equivalent, and were negligible for ^{238}U and ^{232}Th. Ages were determined using the decay constants of Cheng et al. (2000). Ages and errors were calculated using Isoplot (Ludwig, 2003).

Relatively high concentrations of ^{232}Th in the speleothem (~1 to 15 ppb, median 4.2 ppb) indicate the presence of silicate detritus, likely derived from windblown dust or soil above the cave. As discussed by Hellstrom (2006), limiting values for initial isotopes of U and Th consistent with preservation of stratigraphic order may be derived from a sequence of speleothem samples with varying $^{230}Th/^{232}Th$ ratios. We have corrected for U and Th isotopes contributed by detritus assuming activity ratios of $(^{232}Th/^{238}U) = 1.45 \pm 0.35$, $(^{230}Th/^{238}U) = 1.0 \pm 0.25$, and $(^{234}U/^{238}U) = 1.0 \pm 0.25$. Uncertainties associated with the detritus correction were propagated through to the age.

3.3. Stable isotope analyses

Stable isotope samples (25 to 75 µg) were microdrilled from thick sections along the growth axis of MC3-A using a fully automated Merchantek microdrilling system with ~50 µm spatial resolution. Stable isotope samples were roasted at 375 °F *in vacuo* to remove organic volatiles. $\delta^{18}O$ and $\delta^{13}C$ values were determined using a Fisons Optima IRMS with a 90 °C Isocarb common acid bath autocarbonate system in the Stan Margolis Stable Isotope Lab, UC Davis. Values are reported relative to Pee Dee Belemnite (PDB) using standard delta notation; analytical precision for both $\delta^{18}O$ and $\delta^{13}C$ is $<\pm 0.1‰$ (1σ). $\delta^{18}O$ and $\delta^{13}C$ profiles were also completed for dated intervals of MC3-B and C in order to facilitate the correlation of U-series samples between cores.

3.4. Trace element and Sr isotope analyses

Trace element analyses were carried out by laser ablation ICPMS using an Agilent 7500 series quadrupole ICPMS coupled to a New Wave Research UP-213 ablation system at the Interdisciplinary Center for Plasma Mass Spectrometry, UC Davis. Measurements were made on thick (~400 µm) polished sections using a 20 µm spot size and 80 µm spacing.

Additionally, speleothem, microsampled at a 1 mm intervals, and host calcites were processed for Sr isotope analysis using chemical pretreatments to remove Sr associated with absorbed or included noncarbonate phases (Montañez et al., 2000). Samples of soils above Moaning Cave were leached with progressively stronger solutions (1 M ammonium acetate, 4% acetic acid, concentrated (48 M) hydrofluoric acid) in order to characterize the $^{87}Sr/^{86}Sr$ ratio of leachable Sr in soil components (carbonate, volcanic grains, and phyllosilicates). $^{87}Sr/^{86}Sr$ ratios were measured in solution mode on a Nu MC-ICPMS in the Geology Department at UC Davis and values were normalized to a nominal value for SRM987 of 0.710248.

4. Results

U-series ages preserve stratigraphic order, and ages for two samples (MC8A) from the same speleothem layer in core MC3-B show excellent reproducibility (Table 1; Fig. 2), consistent with a closed $^{238}U/^{234}U/^{230}Th$ system in the speleothem since precipitation. MC8B, taken from the correlative position in core MC3-C, yields the same age as MC8A (10.37 ± 0.25 ka and 10.30 ± 0.18 ka, respectively), supporting the correlations among cores. U-series ages for MC3 range from 16.5 to 8.8 ka, indicating that the isotopic and trace element time series span the latest glacial period through early Holocene. In MC3-A, the average growth rate is relatively rapid (16.4 µm/year) between 16.5 and 14.9 ka, slows to 6.0 µm/year between 14.9 and 12.3 ka during the Bølling–Allerød (B–A), and at 12.3 ka, increases again to

Table 1
$^{230}Th/U$ analytical data and ages for MC3 speleothem.

Sample	Depth (mm)	Wt (mg)	U (ppm)	^{232}Th (ppm)	$^{230}Th/^{232}Th$	Measured $^{230}Th/^{238}U$	Measured $^{234}U/^{238}U$	Uncorrected ^{230}Th age (ka)	Corrected ^{230}Th age (ka)	Initial $^{234}U/^{238}U$
MC1	9	274.5	0.302	0.00281	28.2	0.08672 ± 0.0011	1.097 ± 0.0034	8.98 ± 0.12	8.77 ± 0.14	1.099 ± 0.003
MC9	18	515.2	0.465	0.00473	26.1	0.08753 ± 0.0009	1.091 ± 0.0065	9.12 ± 0.11	8.89 ± 0.14	1.094 ± 0.007
MC8A(1)	21.3	401.5	0.473	0.00418	34.5	0.1004 ± 0.0016	1.093 ± 0.0026	10.51 ± 0.18	10.31 ± 0.19	1.095 ± 0.003
MC8A(2)	21.3	450.7	0.458	0.00402	34.4	0.09958 ± 0.0014	1.086 ± 0.0048	10.49 ± 0.16	10.29 ± 0.18	1.089 ± 0.005
MC8B	21.3	413.5	0.456	0.00424	33.0	0.1011 ± 0.0022	1.093 ± 0.0052	10.58 ± 0.24	10.37 ± 0.25	1.096 ± 0.005
MC 4-1		436.3	0.463	0.01300	11.7	0.1081 ± 0.0021	1.093 ± 0.0087	11.36 ± 0.25	10.72 ± 0.34	1.096 ± 0.009
MC 4-2		532.8	0.461	0.00664	22.3	0.1059 ± 0.0023	1.092 ± 0.0044	11.12 ± 0.26	10.79 ± 0.28	1.095 ± 0.005
MC5B	22.5	356.5	0.457	0.00733	19.7	0.1042 ± 0.0037	1.069 ± 0.0044	11.19 ± 0.42	10.82 ± 0.44	1.071 ± 0.005
MC3	23	391.8	0.493	0.0108	16.6	0.1198 ± 0.0026	1.094 ± 0.0016	12.64 ± 0.30	12.14 ± 0.35	1.098 ± 0.002
MC5	25	401.9	0.443	0.0158	10.3	0.1208 ± 0.0029	1.068 ± 0.0037	13.09 ± 0.34	12.26 ± 0.45	1.071 ± 0.004
MC10	41	803.5	0.168	0.00164	44.4	0.1425 ± 0.0017	1.098 ± 0.0036	15.14 ± 0.21	14.92 ± 0.22	1.103 ± 0.004
MC 4-4		663.0	0.127	0.00090	65.9	0.1547 ± 0.0016	1.102 ± 0.0064	16.48 ± 0.21	16.32 ± 0.22	1.107 ± 0.007
MC2	67	330.5	0.174	0.00093	88.3	0.1564 ± 0.0030	1.105 ± 0.0025	16.63 ± 0.35	16.51 ± 0.35	1.110 ± 0.003
MC 4-5		473.9	0.146	0.00527	13.6	0.1626 ± 0.0036	1.084 ± 0.0063	17.71 ± 0.44	16.88 ± 0.53	1.089 ± 0.007

All isotope ratios are given as activity ratios; errors are 2σ. Activity ratios used for detritus correction are $(^{232}Th/^{238}U) = 1.45 \pm 0.35$, $(^{230}Th/^{238}U) = 1.0 \pm 0.25$, and $(^{234}U/^{238}U) = 1.0 \pm 0.25$. Decay constants used are from Cheng et al., 2000. Initial $^{234}U/^{238}U$ calculated from present day, detritus-corrected $^{234}U/^{238}U$ and corrected ^{230}Th age. Samples MC8A(1), MC8A(2), and MC9 were taken from Core MC3-B. Samples MC5B, MC8B, and MC10 were taken from Core MC3-C. Corresponding depths in Core MC3-A are given. Weighted mean age of samples MC8A(1), MC8A(2), and MC8B used for age model is 10.32 ± 0.21 ka. Samples MC 4-1 through MC 4-5, taken from Core MC3-D, are not included in the age model, but were used to determine the $(^{232}Th/^{238}U)$ for detritus correction.

Please cite this article as: Oster, J.L., et al., Late Pleistocene California droughts during deglaciation and Arctic warming, Earth Planet. Sci. Lett. (2009), doi:10.1016/j.epsl.2009.10.003

16.7 μm/year following the onset of the Younger Dryas (YD) (Fig. 3). For the interval of rapid growth rate between 16.5 and 14.9 ka, the stalagmite exhibits fibrous and elongate columnar fabrics indicative of continuous precipitation under relatively high and consistent drip rates, low $CaCO_3$ supersaturation, and near fluid–carbonate equilibrium conditions (Frisia et al., 2000). Similar fabric is observed for the interval 12.3 to 12.1 ka, suggesting a possible second brief period of increased growth rates during the initial YD. For the interval 14.9 to12.3 ka where average growth rate slowed by >50%, the elongate columnar fabric is intercalated with mm-scale intervals of microcrystalline calcite, which are characteristic of intermittent growth under variable flow conditions and elevated influx of detrital and/or colloidal particles (Frisia et al., 2000). Following an inferred increase in average growth rate between 12.3 and 12.1 ka, growth rate in MC3-A decreases dramatically to 0.4 μm/year between 12.1 and 10.8 ka. The stalagmite continues to display elongate columnar fabric during this interval, however breaks in the crystal growth pattern and a possible dissolution surface suggest the calculated average growth rate has large uncertainty. Growth rates in MC3-B and C are estimated to be 100 to 200% greater (0.8 to 1.1 μm/year) than for MC3-A during this interval. For the interval 10.8 to 8.9 ka, the average growth rate in MC3-A increases to 2.4 μm/year before rising dramatically to 75 μm/year between 8.9 and 8.8 ka. During this interval, the stalagmite again exhibits an elongate columnar fabric intercalated with mm-scale intervals of microcrystalline calcite.

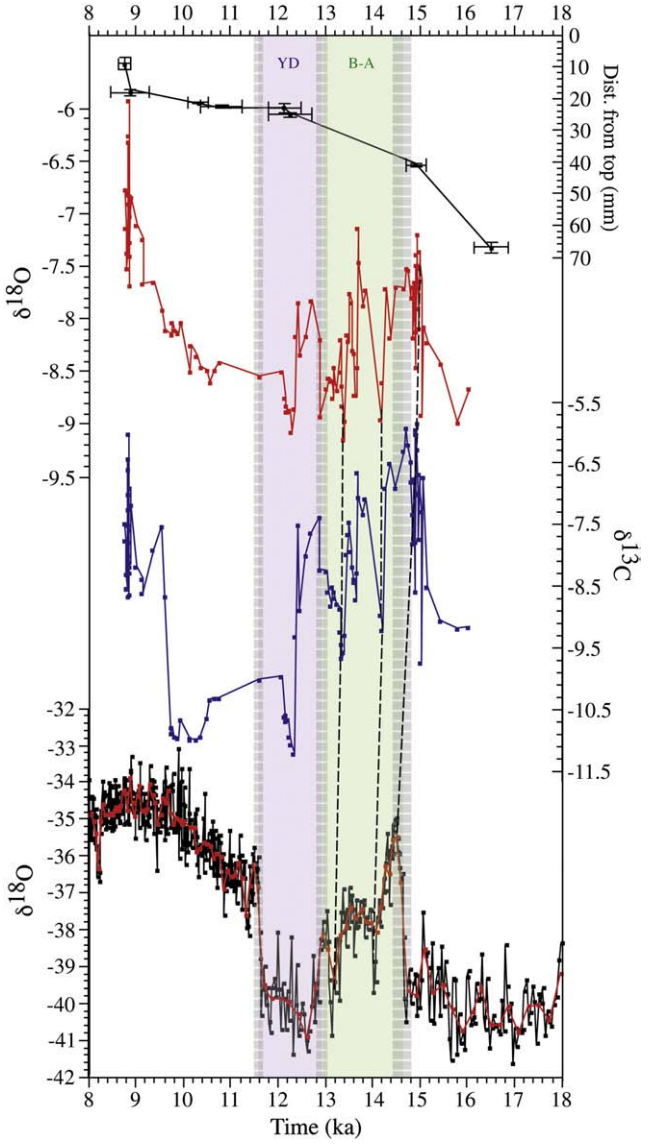

Fig. 3. Comparison of Moaning Cave $\delta^{18}O$ (top) and $\delta^{13}C$ with GISP2 $\delta^{18}O$ (Stuiver and Grootes, 2000). Red line is 5 pt running mean of GISP2 data. Bølling–Allerød and Younger Dryas intervals in GISP2 record are shaded, respectively, green and purple. Widths of gray bars indicate uncertainties in the GISP2 age model. Black boxes show U-series ages and errors (2σ) of Moaning Cave samples. Black dashed lines tie the onset of the Bølling, the Older Dryas, and the Inter-Allerød Cold Period intervals in both records. MC $\delta^{18}O$ values have been corrected for changes in seawater $\delta^{18}O$ with sea level using Fleming et al., 1998.

The Moaning Cave stalagmite $\delta^{18}O$ time series exhibits systematic fluctuations between −7.0‰ and −9.7‰, while $\delta^{13}C$ fluctuates over a larger range (−5.9‰ and −11.2‰) and records several large shifts that generally coincide with $\delta^{18}O$ fluctuations (Fig. 3). Mickler et al. (2004, 2006) showed that non-equilibrium fractionation of stable isotopes can occur during speleothem growth due to rapid and extended degassing of CO_2 driven by decreased seepage water flow rates, increased evaporation, and/or changing cave air–water CO_2 ratios. Such kinetic effects lead to ^{13}C- and ^{18}O-enrichment in the speleothem and elevated concentrations of trace elements such as Mg, Sr, and Ba (Lorens, 1981).

Moaning Cave $\delta^{18}O$ and $\delta^{13}C$ values exhibit significant down-axis correlation ($r^2 = 0.81$) that could be interpreted to record non-equilibrium isotope precipitation (e.g., Mickler et al., 2006). However, the values and patterns in $\delta^{18}O$ and $\delta^{13}C$ between 12.3 and 9.6 ka in MC3-A are reproducible in two other cores (MC3-B and C) taken off the growth axis through the same stalagmite. If kinetic effects were dominating the Moaning Cave record, $\delta^{18}O$ values, in particular, would be expected to vary substantially perpendicular to the growth axis (Hendy, 1971); rather than the good agreement observed in $\delta^{18}O$ values for on- and off-axis samples from the same layer. Furthermore, similar down-axis correlation between $\delta^{18}O$ and $\delta^{13}C$ has been observed in other speleothem records and interpreted to reflect climatic processes rather than non-equilibrium calcite precipitation (e.g. Genty et al., 2003; Frappier et al., 2007), Similar *long-term* trends in MC3 $^{87}Sr/^{86}Sr$ and trace element concentrations (see below), in particular through the late glacial and B–A, also argue against a significant influence of kinetic effects given the negligible environmental fractionation of $^{87}Sr/^{86}Sr$ values (Banner et al., 1996).

MC3 [Mg] varies between 1800 and 9000 ppm, [Sr] between 25 and 85 ppm, and [Ba] between 3 and 7 ppm. $^{87}Sr/^{86}Sr$ values vary between 0.70577 and 0.70689. Overall, changes in [Mg], [Sr], and [Ba] and $^{87}Sr/^{86}Sr$ values through the late glacial and the first half of the YD (~12.4 to ~12.2 ka) define general trends similar to those delineated by the stable isotope time series, with intervals of low trace element concentrations and less radiogenic $^{87}Sr/^{86}Sr$ values generally coincident with the most negative $\delta^{18}O$ and $\delta^{13}C$ values (Fig. 4). This trend of positively covarying stable isotope and geochemical proxies is interrupted between 10.6 and 9.4 ka by a shift to a generally inverse relationship between trace elements and $\delta^{13}C$ (Table 2). From 9.4 to the end of the record (8.8 ka), there is a return to positive correlation between proxies, though the correlations are less pronounced.

5. Evaluation of paleoclimate and paleohydrology time series

In the following section, we first evaluate the processes that affect speleothem $\delta^{18}O$, $\delta^{13}C$, [Mg], [Sr], [Ba], and $^{87}Sr/^{86}Sr$ in the context of the MC3 time series. Subsequently, we discuss the climatic and hydrologic interpretations for the Moaning Cave record in three time intervals, 16.5–10.6 ka, 10.6–9.4 ka, and 9.4–8.8 ka. These intervals are defined by distinct changes in the correlations among isotopic and trace element proxies in the speleothem.

5.1. $\delta^{18}O$

MC3 $\delta^{18}O$ variations, which have been corrected for changes in seawater $\delta^{18}O$ (cf., Vacco et al., 2005) using the record of deglacial sea-level rise (Fleming et al., 1998), can be interpreted as changes in surface air temperature and/or rainfall amount. Present day air temperature

Please cite this article as: Oster, J.L., et al., Late Pleistocene California droughts during deglaciation and Arctic warming, Earth Planet. Sci. Lett. (2009), doi:10.1016/j.epsl.2009.10.003

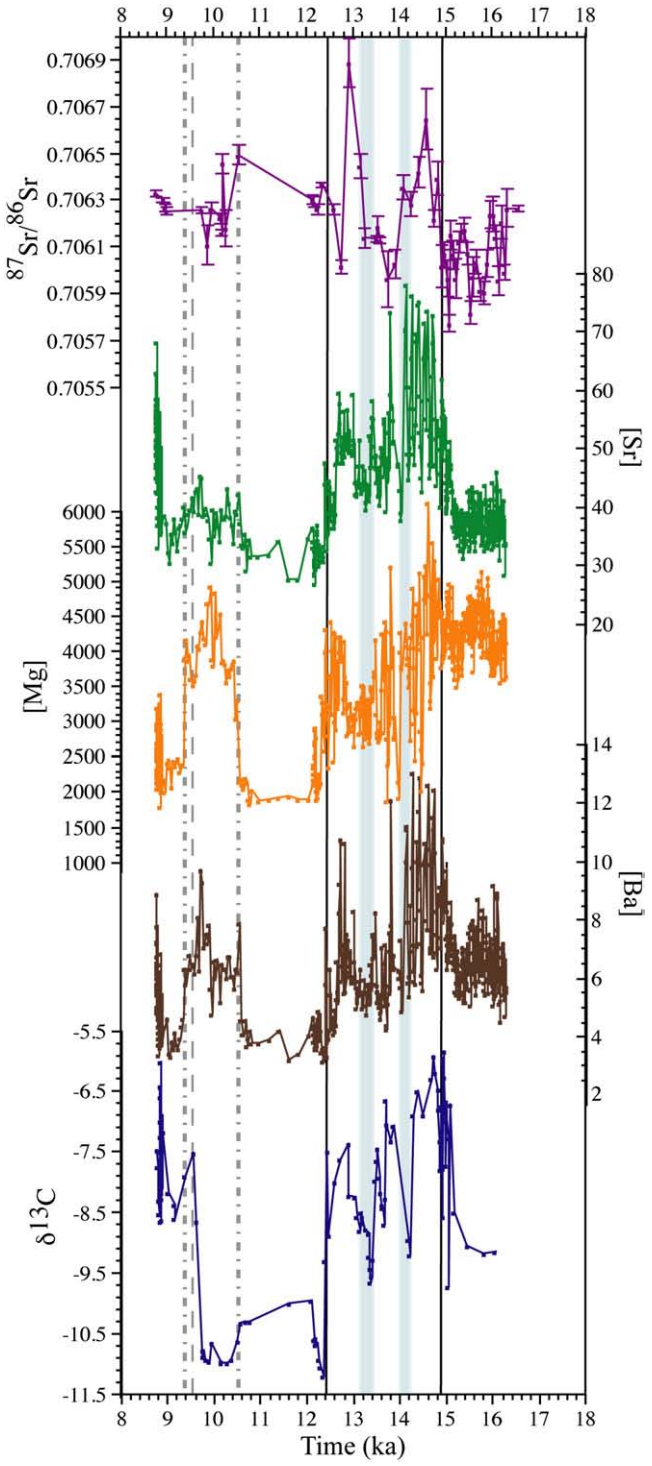

Fig. 4. Comparison of Moaning Cave $^{87}Sr/^{86}Sr$, [Sr], [Mg], [Ba], and $\delta^{13}C$. Onset of the B–A (15 ka) and YD (12.5 ka) in the Moaning Cave $\delta^{13}C$ record are indicated by solid lines. Blue bar indicates the extent of wet conditions above Moaning Cave as shown by the $\delta^{13}C$ record. The end of YD conditions at Moaning Cave at 9.6 ka is shown with a dashed line. Thin gray bars highlight the Older Dryas, and the Inter-Allerød Cold Period intervals. Dash–dotted lines demarcate the interval of potential hydrologic variability between 10.6 and 9.6 ka as indicated by the trace element records. Increases in $\delta^{13}C$ suggest either decreased soil respiration or increased prior calcite precipitation. Increases in [Mg], [Sr], and [Ba] also suggest increased prior calcite precipitation. Increased $^{87}Sr/^{86}Sr$ suggests elevated water rock interactions.

within Moaning Cave varies by 2.3 °C during the year, a variation that could account for only a 0.5‰ change in the $\delta^{18}O$ of speleothem calcite (using the equilibrium fractionation relationship of Kim and O'Neil, 1997). Furthermore, more stable cave air temperature variations would be expected prior to artificial ventilation of the cave (1922). Thus, we interpret the oxygen isotope values in Moaning Cave speleothems to primarily record the $\delta^{18}O$ value of drip water and thus the $\delta^{18}O$ of precipitation falling above the cave (Dorale et al., 1998; McDermott, 2004). Precipitation $\delta^{18}O$ is related to changes in continental ice volume, surface air temperature, moisture source, rainfall amount, and evaporation (Dansgaard, 1964; Vaks et al., 2003). Although we discount changes in cave air temperature as the source of variation in MC3 $\delta^{18}O$, the observed shifts (up to 2‰) could suggest surface air temperature changes of 1 to 4 °C, using the range of 0.5–0.7‰/°C for $\delta^{18}O$ in precipitation proposed by Rozanski et al. (1993), if no other effects were influencing precipitation $\delta^{18}O$. Furthermore, there is no reason to believe that the source of moisture to the Sierra Nevada foothills changed on these timescales, as it is unlikely that the North American Monsoon, which currently affects the southwestern United States, extended this far to the north and west during the last glacial period (Adams and Comrie, 1997). Additionally, precipitation amount effects on $\delta^{18}O$ would lead to more negative $\delta^{18}O$ when rainfall amounts are higher (Dansgaard, 1964).

5.2. $\delta^{13}C$ and trace element concentrations

Variations in MC3 $\delta^{13}C$ are most likely due to shifts in the amount of soil-derived CO_2 contributed to seepage waters and/or changes in calcite precipitation up-flow from the stalagmite drip site. Soil respiration rates above Moaning Cave likely decreased during dry periods, leading to decreased contribution of soil CO_2 to seepage water DIC and more positive speleothem $\delta^{13}C$ values (e.g. Quade et al., 1989; Genty et al., 2003; Cruz et al., 2006). Conversely, soil respiration could have been at its maximum during wet periods, leading to minimum values of seepage water DIC $\delta^{13}C$. Furthermore, the lack of pollen or packrat midden evidence for C_4 flora in the greater study region over the past 20+ ky (Cole, 1983; Thompson et al., 1993; Davis, 1999) argues against changes in the C_3:C_4 plant ratios leading to changes in soil-derived $\delta^{13}C$ above Moaning Cave (Dorale et al., 1998).

Variations in $\delta^{13}C$, as well as [Mg], [Sr], and [Ba] in MC3 are also likely controlled through most of the record by variations in the amount of calcite precipitated in the aquifer up-flow from the speleothem drip site (prior calcite precipitation). As CO_2 is degassed from drip water, the lighter $^{12}CO_2$ molecule is preferentially released, leading to more positive $\delta^{13}C$ in the remaining drip water. Likewise, as calcite is precipitated from drip water, the remaining water possesses higher [Mg], [Sr], and [Ba], as the distribution coefficients for these elements in calcite are much less than 1 (Lorens, 1981; Fairchild et al., 2000). Prior calcite precipitation in a cave will increase due to increased evaporation or degassing or slower seepage rates that allow saturation to be reached

Table 2
Correlation coefficients for proxies by time period.

Proxies	8.8–9.4 (ka)	9.4–10.6 (ka)	10.6–16.5 (ka)
$\delta^{13}C$ vs $\delta^{18}O$	0.85	0.82	0.88
$\delta^{13}C$ vs [Mg]	0.11	−0.36	0.66
$\delta^{13}C$ vs [Sr]	0.30	0.11	0.80
$\delta^{13}C$ vs [Ba]	0.26	−0.19	0.76
$\delta^{18}O$ vs [Mg]	0.14	0.00	0.55
$\delta^{18}O$ vs [Sr]	0.03	0.16	0.60
$\delta^{18}O$ vs [Ba]	0.04	0.05	0.64
[Mg] vs [Sr]	0.37	−0.13	0.57
[Mg] vs [Ba]	0.36	0.41	0.79
[Sr] vs [Ba]	0.94	0.72	0.87

Proxy r^2 values were calculated by interpolating proxy records onto one age model using the ARAND software package (Howell et al., 2006). Correlation coefficients were not calculated for $^{87}Sr/^{86}Sr$ with the other proxies given that the resolution of the $^{87}Sr/^{86}Sr$ record is much lower.

Please cite this article as: Oster, J.L., et al., Late Pleistocene California droughts during deglaciation and Arctic warming, Earth Planet. Sci. Lett. (2009), doi:10.1016/j.epsl.2009.10.003

earlier in the water travel path (Fairchild et al., 2000). Slower seepage rates, and therefore increased groundwater residence times, would occur during periods of increased aridity resulting in decreased water supply to the cave. In addition, increased evaporation and degassing of drip waters may arise during periods of increased cave air ventilation. When surface air temperatures are relatively low, cold, dense outside air will sink into the cave, displacing warmer, high pCO_2 cave air and leading to an overall decrease in cave air pCO_2 (Banner et al., 2007). In this scenario, increased degassing and prior calcite precipitation driven by decreased cave air pCO_2 would have occurred in Moaning Cave during colder periods. This relationship, however, is not consistent with the observed positive correlation between $\delta^{18}O$ and $\delta^{13}C$ (Table 2; Fig. 3). Rather, the strong covariation between $\delta^{18}O$, $\delta^{13}C$, [Mg], [Sr], and [Ba] during periods of increased warming over Greenland favors an increase in prior calcite precipitation, probably due to decreased seepage rates and increased groundwater residence time during dry periods in the central Sierra Nevada.

Variation in [Mg] in the Moaning Cave speleothem might also result from differential dissolution of limestone and dolomite in the dolomite-bearing marble host-rock (Hellstrom and McCulloch, 2000; Fairchild et al., 2000). Dolomite dissolution in the aquifer, however, is not likely the dominant control on [Mg] concentrations given the positive correlation between [Mg], [Sr] and [Ba], as dolomite typically has lower concentrations of Sr and Ba than calcite (Hellstrom and McCulloch, 2000). Additionally, dolomite dissolution would not lead to concurrent variations in $\delta^{13}C$, as dolomite $\delta^{13}C$ is typically rock-buffered to host limestone $\delta^{13}C$ values (Machel et al., 1996). Lastly, given that Moaning Cave is located ~200 km from the coast and there is no evidence of major shifts in wind direction over the region since the last glacial period, the contribution of [Sr] and [Ba] from sea spray and dust to the Moaning Cave record should be relatively constant (Ayalon et al., 1999). Thus, we conclude that variations in prior calcite precipitation due to changes in groundwater residence time are most likely the dominant control on Moaning Cave trace element concentrations throughout much of the record.

5.3. $^{87}Sr/^{86}Sr$

We interpret MC3 $^{87}Sr/^{86}Sr$ ratios to reflect varying contributions from two end-members characterized in this study: a less radiogenic soil source with a value of 0.70459 ± 16 derived from the weathering of metamorphic and altered volcanic rocks above Moaning Cave and a more radiogenic host-marble source with a value of 0.70745 ± 9 (Fig. 5). Previous studies of Sr isotopes in speleothems have interpreted increases in host-rock derived Sr as representing periods of increased residence time and drier climates (e.g. Banner et al., 1996), and we interpret the Moaning Cave Sr isotopic record similarly. During periods of increased precipitation, rapidly infiltrating water would have produced drip waters with less radiogenic Sr reflecting increased contribution of soil-dominated Sr. During drier periods increased seepage water residence time in the carbonate aquifer and increased meteoric water–marble interactions would have led to more radiogenic speleothem Sr.

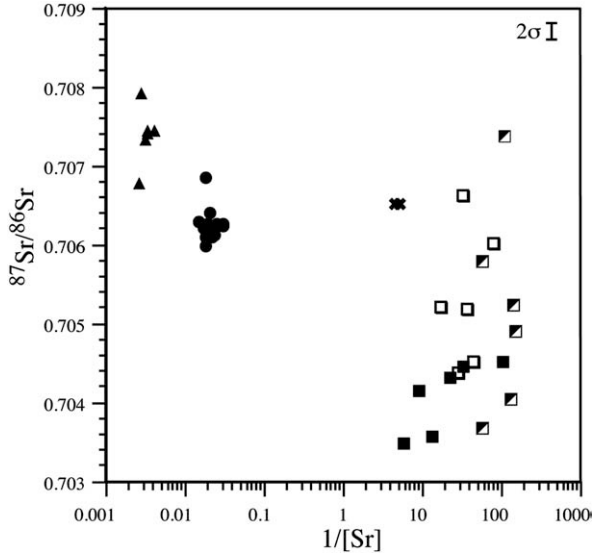

Fig. 5. $^{87}Sr/^{86}Sr$ vs. 1/[Sr] for host limestone (triangles), speleothems (circles), spring water (x) and soil prewash (open squares), acetic acid (half-filled squares), and HF (black squares) leachates. Error bar for $^{87}Sr/^{86}Sr$ is shown. Errors for [Sr] are smaller than the symbols.

5.4. The Moaning Cave record from 16.5 to 10.6 ka

From 16.5 to 10.6 ka stable isotope and geochemical proxies are positively correlated ($r^2 = 0.55$ to 0.88; Table 2). $\delta^{18}O$ and $\delta^{13}C$ values rise abruptly at 15 ka, coincident (within dating errors of about ± 220 years in the MC3 record) with the onset of the Bølling–Allerød (B–A) warm period in the GISP2 ice core (14.7 ± 0.29 ka) (Meese et al., 1997; Stuiver and Grootes, 2000). When temperatures in Greenland were warm during the Bølling and early and late Allerød periods, $\delta^{18}O$, $\delta^{13}C$, [Mg], [Sr], and [Ba] increased in the speleothem coincident with shifts to more radiogenic $^{87}Sr/^{86}Sr$ values. Less negative $\delta^{18}O$ values suggest potentially warmer surface air temperatures above Moaning Cave, increased evaporation, and/or an overall decrease in precipitation occurred at these times. Increased $\delta^{13}C$ values suggest either a decrease in vegetation leading to less contribution of soil CO_2 to cave water, increased prior calcite precipitation, or the interaction of both processes. Increases in trace element concentration further support increased prior carbonate precipitation during warm periods. This, coupled with more radiogenic $^{87}Sr/^{86}Sr$, suggests increased contribution of solution metals from interaction with the host-rock relative to soil water. All of these parameters are consistent with a drier and possibly warmer climate above Moaning Cave during Greenland warm periods between 16.5 and 12.2 ka.

Conversely, abrupt shifts to lower $\delta^{18}O$, $\delta^{13}C$, and [Mg], [Sr], and [Ba] and less radiogenic $^{87}Sr/^{86}Sr$ values at ~14.2 ka and ~13.4 ka, which may be coincident with the Older Dryas (~14 ka), and the Inter-Allerød Cold period (13.1 ka) as defined in GISP2, are consistent with shifts to wetter and possibly colder conditions above Moaning Cave. An abrupt shift to the lowest $\delta^{18}O$, $\delta^{13}C$, [Mg], [Sr], and [Ba] values in MC3 occurs at 12.4 ka, coincident within dating error (± 450 years) with the onset of the YD. These shifts, as well as a synchronous increase in average growth rate from 6.0 to 16.7 μm/year at this time, are consistent with wetter climatic conditions on the western slope of the central Sierra Nevada at the onset of the YD.

Following the initial decrease into the YD, $\delta^{18}O$ and $\delta^{13}C$ and trace element values increase slightly at ~12.2 ka. $^{87}Sr/^{86}Sr$ values also increase slightly at this time. These changes suggest a decrease in the contribution of soil-respired CO_2 to seepage waters and an increase in prior calcite precipitation coupled with increased water–host-rock interactions, consistent with a slight mid-YD increase in aridity and possibly temperature in this region.

5.5. Evidence for a shift in drip center at 12.1 ka

Following the slight increase in all of the proxy records at 12.2 ka, the average growth rate between 12.1 and 10.8 ka in MC3-A falls dramatically to 0.4 μm/year, while slightly to significantly greater average growth rates occur in synchronous intervals of MC3-B (3.9 μm/year between 12.3 and 10.3 ka) and MC3-C (1.1 μm/year between 12.1 and 10.8 ka) (Table S1). $\delta^{18}O$, $\delta^{13}C$, and [Mg], [Sr], and [Ba] become stable at this time, with [Mg], [Sr], and [Ba] at minimum values, and $\delta^{18}O$ and $\delta^{13}C$ at slightly more positive values.

Please cite this article as: Oster, J.L., et al., Late Pleistocene California droughts during deglaciation and Arctic warming, Earth Planet. Sci. Lett. (2009), doi:10.1016/j.epsl.2009.10.003

The large decrease in growth rate in MC3-A between 12.1 and 10.8 ka could be interpreted to suggest decreased drip rate due to increased aridity above the cave or changes in ventilation and cave air pCO_2 (e.g. Musgrove et al., 2001; Banner et al., 2007). Speleothem growth rates are typically inversely correlated with cave air pCO_2, which varies with seasonal differences between cave and surface air temperatures (Banner et al., 2007). Thus, the dramatic decrease in MC3-A growth rate at 12.1 ka could indicate decreased ventilation due to increased surface air temperatures between 12.1 and 10.8 ka. The relatively light $\delta^{18}O$ values during this interval, however, suggest surface air temperatures did not significantly increase. Furthermore, textural evidence of a discontinuity in MC3-A and migration of the highest growth rates observed in this interval (12.1 and 10.8 ka) to MC3-B indicates that, rather than an overall decrease in drip rate, the drip center of the Moaning Cave stalagmite shifted at ~12.1 ka. A break in the crystal growth pattern with a possible dissolution surface and numerous fluid inclusions during this interval in MC3-A further supports this hypothesis. This surface is present to a lesser degree in MC3-C and is not discernable in MC3-B. Lastly, the continued low $\delta^{13}C$, [Mg], [Sr], and [Ba] indicate that a wet climate persisted above Moaning Cave between 12.1 and 10.8 ka. Thus, a shift in drip center away from the part of the speleothem sampled in MC3-A best accounts for the observed growth rate changes in this interval.

5.6. The Moaning Cave record from 10.6 to 9.4 ka

At 10.6 ka, $\delta^{18}O$ values fall slightly and $\delta^{13}C$ reach their minimum in the Moaning Cave record, coincident with an abrupt increase in [Mg]. These shifts are accompanied by slight increases in [Ba] and [Sr] and a slight shift in $^{87}Sr/^{86}Sr$ to more radiogenic values.

The [Mg] increase could represent a shift to a more Mg-rich source within the aquifer. The Moaning Cave host carbonate consists of metamorphosed limestones and dolomites (Clark and Lydon, 1962; Bowen, 1973). Thus, a change in groundwater routing could have led to increased fluid interaction with a more dolomite-rich (Mg-rich) portion of the host-rock. If, however, this very large increase in [Mg] was produced through the increased residence time/prior calcite precipitation mechanism suggested for the earlier part of the MC3 record, a coincident large increase in $\delta^{13}C$ would be expected, but is not observed. Furthermore, the lack of a change in the crystal structure or in inclusion density during this interval indicates that the abrupt increase in trace element concentrations is not related to the presence of contaminating phases in the speleothem. [Sr] and [Ba] also increase at this time, but not to the same degree as the shift in [Mg]. These changes are consistent with a shift to a dolomitic source, as dolomite contains less Sr and Ba than calcite (Hellstrom and McCulloch, 2000). Thus, we argue that the large increase in [Mg], coupled with the smaller increases in [Sr] and [Ba], and the near-minimum $\delta^{13}C$ values are best explained by a change in groundwater flow path that does not necessitate a climatic shift to drier conditions above Moaning Cave.

At 9.6 ka, $\delta^{13}C$ values increase abruptly from approximately −11‰ to −7.5‰, suggesting a rapid shift to a drier, and possibly warmer climate above Moaning Cave. At this time, $\delta^{18}O$ values continue to gradually rise, suggesting that either air temperature increases above Moaning Cave were more gradual than precipitation changes or that vegetation above the cave reached a soil moisture threshold that led to a rapid decrease in vegetation density at 9.6 ka (e.g. deMenocal et al., 2000).

5.7. The Moaning Cave record from 9.4 to 8.8 ka

At ~9.4 ka, [Mg] and [Ba] decrease abruptly, while [Sr] falls more gradually. Following this, $\delta^{13}C$, [Mg], [Sr], and [Ba] are again positively correlated though the correlations are less strong than during the earlier part of the MC3 record. Stalagmite growth rate in MC3-A increases dramatically from 2.3 μm/year to 75 μm/year at 8.9 ka; the timing of this growth rate shift, however, is constrained solely by the location of dated samples. This average growth rate increase and the return to positively correlated $\delta^{13}C$, [Mg], [Sr], and [Ba] may suggest that another shift in the flow path supplying the speleothem occurred given the fracture-flow dominated hydrology of the host aquifer. Variations in the proxy records in this portion of MC3 can therefore be interpreted as recording similar variations in rainfall in the region and residence time as occurred during the B–A and early YD. The return to correlated proxies further supports our hypothesis that the lack of correlation between the trace elements and stable isotopes during the interval 10.6 to 9.4 ka records a local shift in hydrology with a shift in drip center.

6. Discussion and summary

The speleothem MC3 records variations in regional climate and local hydrology between 16.5 and 8.8 ka. We interpret elevated $\delta^{18}O$, $\delta^{13}C$, [Mg], [Sr], and [Ba] and more radiogenic $^{87}Sr/^{86}Sr$ to indicate periods of decreased soil-respired CO_2, increased prior calcite precipitation, and increased groundwater–rock interaction above Moaning Cave. In turn, we attribute these proxy behaviors to relatively dry and possibly warm conditions at Moaning Cave during the Bølling, and early and late Allerød warm periods noted in the Greenland ice core records. Conversely, lower $\delta^{18}O$, $\delta^{13}C$, [Mg], [Sr], and [Ba] and less radiogenic $^{87}Sr/^{86}Sr$ record elevated soil-respired CO_2, decreased prior calcite precipitation, and more limited water–rock interaction presumably in response to increased precipitation above Moaning Cave during the colder Older Dryas, Inter-Allerød Cold Period, and YD.

Studies of lacustrine, glacial, and speleothem records in western North America have documented sub-centennial to millennial shifts in mid-latitude western North American continental climate since the late Pleistocene, similar to those seen in the early part of the Moaning Cave record (e.g., Gosse et al., 1995; Clark and Bartlein, 1995; Benson et al., 1996, 1997, 1998; Lin et al., 1998; Benson et al., 2003; Polyak et al., 2004; Brook et al., 2006; Ellwood and Gose, 2006). These records, however, present an inconsistent picture of how regional climate changes in western North America with distal warmings and coolings in the North Atlantic during the late Pleistocene, and the YD in particular. In some studies late Pleistocene cooling events in the North Atlantic region (e.g., stades of D–O and, B–A, YD) have been correlated to cool but dry climates in the Sierra Nevada and western Great Basin regions (e.g., Benson et al., 1997, 1998, 2003; Clark, 2003). For example, there is no evidence for a YD glacial advance on the east side of the Sierra Nevada (Clark and Gillespie, 1997; Phillips et al., 2009). In contrast, other studies indicate possible increases in effective moisture during the YD in parts of the Great Basin attributed to a southward displacement of the polar jet stream (Mensing, 2001; Polyak et al., 2004; Oviatt et al., 2005; MacDonald et al., 2008). Other records lack sufficient temporal resolution to definitively establish (or refute) the synchrony of regional climate oscillations with the near-global YD event (Mensing, 2001 and references within; Owen et al., 2003; Winograd et al., 2006) (Fig. 1). These disparities confound the issue of whether actual differences in regional climatic response to distal climate events noted in the northern high-latitudes occurred.

Notably, MC3 provides a high-resolution continuous record through this interval that is consistent with *increased* effective moisture in the central Sierra Nevada during past cool periods (Older Dryas, Inter-Allerød Cold Period, onset of the Younger Dryas) and significantly drier conditions during past warmings (Bølling, early and late Allerød). Such a pattern is consistent with recent models of the impact of greenhouse-gas forcing on regional climates (Sewall and Sloan, 2004; Sewall, 2005; Seager et al., 2007). Western North American-focused simulations highlight the sensitivity of Pacific-sourced winter storm tracks and precipitation levels in mid-latitude western North America to changes in Arctic sea ice extent and atmospheric cell stability expected with global warming. Decreased Arctic sea ice leads to a northward deflection of the polar jet stream and with it the present path of winter storms. In regions such as northern California that are already characterized by

Please cite this article as: Oster, J.L., et al., Late Pleistocene California droughts during deglaciation and Arctic warming, Earth Planet. Sci. Lett. (2009), doi:10.1016/j.epsl.2009.10.003

marginally sufficient water resources, this effect could translate to significant (up to 30%) reductions in mean annual precipitation relative to current levels (Sewall and Sloan, 2004; Sewall, 2005).

The MC3 time series document a shift to slightly drier conditions at 12.2 ka followed by a potential change in the local hydrology including movement of the stalagmite drip center at 12.1 ka. A shift to drier conditions in the middle of the YD interval has been noted in a number of paleoclimate records in western North America, including diatom and stable isotope records from lakes just east of the Sierra Nevada crest (MacDonald et al., 2008), and sedimentological, stable isotope and pollen records from Owens Lake in the eastern Sierra Nevada (Benson et al., 1997; Mensing, 2001; Benson et al., 2002; Bacon et al., 2006). Additionally, a short-lived increase (0.4‰) in the $\delta^{18}O$ values of the foraminifera *N. Pachyderma* is noted in Santa Barbara Basin (Fig. 1) sediments at ~12.3 ka, indicating a small increase in surface water temperatures off the California coast (Hendy et al., 2002) coincident with the climatic shift on the western slope of the central Sierra Nevada. Mid-YD shifts to warmer conditions have also been noted in other Northern Hemisphere locations, including the GRIP ice core $\delta^{18}O$ record (2‰ increase in at 12.2 ka) (Dansgaard et al., 1993), speleothems from southern France and northern Tunisia (12.2 ka; Genty et al., 2006), and a German lacustrine ostracod record (von Grafenstein et al., 1999). Moreover, while the drip center shift seen in MC3 was most likely caused by a very localized hydrologic change, it is possible that it was initiated by the slight drying noted in the Moaning Cave record at 12.2 ka, which in turn might be linked with the mid-YD warming observed throughout the Northern Hemisphere. It is also worth emphasizing that these hydrologic shifts above Moaning Cave had dramatic effects on trace element records, and this may have important implications for the interpretation of such records from other caves.

Despite the influence of a change in seepage water routing on the MC3 trace element records, the stable isotope records remain low throughout the period 10.6 to 9.6 ka, with $\delta^{13}C$ at its most negative values, arguing for dense vegetation and a relative increase in precipitation until 9.6 ka. Therefore, the Moaning Cave record suggests that wet and possibly colder conditions persisted on the western slope of the central Sierra Nevada well beyond the end of the YD in GISP2 (~11.5 ka). This is an intriguing observation and warrants further evaluation in other continental records from western North America. By 9.0 ka, stable isotopes and trace elements suggest that conditions above Moaning Cave were as dry as those at the onset of the Bølling period.

Our interpretation of the MC3 record indicates that, since the last glacial maximum, warmer episodes in the Sierra Nevada region of central California were associated with decreased levels of effective moisture. Dating of the MC3 time series shows that marked climate fluctuations in the Sierra Nevada region occurred in as little as a few decades, and that one such shift at ~12.4 ka coincided, within the limits of dating, with abrupt climate shifts that occurred globally at the onset of the Younger Dryas climatic event. Past climate shifts in the Sierra Nevada, as elsewhere, occurred in response to modified atmospheric circulation patterns likely driven by northern high-latitude climate anomalies. Such climate shifts persisted throughout the deglaciation despite evolving boundary conditions (e.g. ice sheet extent and volume). The clear expression of the onset of the Younger Dryas, the short-lived drying during the mid-YD and the expression of the Older Dryas and Inter-Allerød Cold Period in the MC record is therefore consistent with recent climate models that highlight the possible importance of such atmospheric teleconnections for California's future climate under conditions of continued global warming and loss of Arctic ice. If this hypothesis is correct, such linkages indicate that in response to global warming, effective moisture levels in the Sierra Nevada region may be reduced not only by enhanced evaporation due to warmer local temperatures, but also by reductions in Pacific moisture delivered to the region, thus strongly impacting water resources in a region already characterized by marginally sufficient water resources.

Acknowledgements

We thank Neil Kelley, and Naomi Marks for field assistance. Steven Fairchild, President of the Sierra Nevada Recreation Corporation, provided access to caves and materials. This paper benefited from discussions with Howie Spero and Jay Banner as well as three anonymous Earth and Planetary Science Letters reviewers. This work was supported by a Cave Research Foundation student grant to Jessica Oster and NSF grants NSF-ATM0823656 to Isabel P. Montañez and Kari M. Cooper, and NSF-ATM0823541 to Warren D. Sharp.

Appendix A. Supplementary data

Supplementary data associated with this article can be found, in the online version, at doi:10.1016/j.epsl.2009.10.003.

References

Adams, D.K., Comrie, A.C., 1997. The North American Monsoon. Bull. Am. Meteorol. Soc. 78, 2197–2213.
Allen, M.R., Ingram, W.J., 2002. Constraints on future changes in climate and the hydrologic cycle. Nature 419, 224–232.
Alley, R.B., Meese, D.A., Shuman, C.A., Gow, A.J., Taylor, K.C., Grootes, P.M., White, J.W.C., Ram, M., Waddington, E.D., Mayewski, P.A., Zielinski, G.A., 1993. Abrupt increase in Greenland snow accumulation at the end of the Younger Dryas event. Nature 362, 527–529.
Ayalon, A., Bar-Matthews, M., Kaufman, A., 1999. Petrography, strontium, barium, and uranium concentrations, and strontium and uranium isotope ratios in speleothems as palaeoclimatic proxies: Soreq Cave, Israel. The Holocene 9, doi:10.1191/095968399673664163.
Bacon, S.N., Burke, R.M., Pezzopane, S.K., Jayko, A.S., 2006. Last glacial maximum and Holocene lake levels of Owens Lake, eastern California, USA. Quat. Sci. Rev. 25, 1264–1282.
Banner, J.L., Musgrove, M., Asmerom, Y., Edwards, R.L., Hoff, J.A., 1996. High-resolution temporal record of Holocene ground-water chemistry: tracing links between climate and hydrology. Geology 24, 1049–1053.
Banner, J.L., Guilfoyle, A., James, E.W., Stern, L.A., Musgrove, M., 2007. Seasonal variations in modern speleothem calcite growth in central Texas, U.S.A. J. Sed. Res. 77, 615–622.
Benson, L., Burdett, J.W., Kashgarian, M., Lund, S.P., Phillips, F.M., Rye, R.O., 1996. Climatic and hydrologic oscillations in the Owens Lake Basin and adjacent Sierra Nevada, California. Science 274, 746–749.
Benson, L., Burdett, J., Lund, S., Kashgarian, M., Mensing, S., 1997. Nearly synchronous climate change in the Northern Hemisphere during the last glacial termination. Nature 388, 263–265.
Benson, L.V., Lund, S.P., Burdett, J.W., Kashgarian, M., Rose, T.P., Smoot, J.P., Schwartz, M., 1998. Correlation of Late-Pleistocene lake-level oscillations in Mono Lake, California, with North Atlantic climate events. Quat. Res. 49, 1–10.
Benson, L., Kashgarian, M., Rye, R., Lund, S., Paillet, F., Smoot, J., Kester, C., Mensing, S., Medo, D., Linström, S., 2002. Holocene multidecadal and multicentennial droughts affecting northern California and Nevada. Quat. Sci. Rev. 21, 659–682.
Benson, L., Lund, S., Negrini, R., Linsley, B., Zic, M., 2003. Response of North American Great Lakes to Dansgaard-Oeschger oscillations. Quat. Sci. Rev. 22, 2239–2251.
Bond, G., Kromer, B., Beer, J., Muscheler, R., Evans, M.N., Showers, W., Hoffman, S., Lotti-Bond, R., Hajdas, I., Bonani, G., 2001. Persistent solar influence on north Atlantic climate during the Holocene. Science 294, 2130–2136.
Bowen, O.E., 1973. The Mineral Economics of the Carbonate Rocks: Limestone and Dolomite Resources of California. California Division of Mines and Geology, Sacramento.
Broecker, W., 2003. Does the trigger for abrupt climate change reside in the ocean or in the atmosphere. Science 300, 1519–1522.
Bromwich, D.H., Toracinta, E.R., Wei, H.L., Oglesby, R.J., Fastook, J.L., Hughes, T.J., 2004. Polar MM5 simulations of the winter climate of the Laurentide Ice Sheet at the LGM. J. Climate 17, 3415–3433.
Bromwich, D.H., Toracinta, E.R., Oglesby, R.J., Fastook, J.L., Hughes, T.J., 2005. LGM summer climate on the southern margin of the Laurentide Ice Sheet: wet or dry? J. Climate 18, 3317–3338.
Brook, G.A., Ellwood, B.B., Railsback, L.B., Cowart, J.B., 2006. A 164 ka record of environmental change in the American Southwest from a Carlsbad Cavern speleothem. Palaeogeogr. Palaeoclimatol. Palaeoecol. 237, 483–507.
Cheng, H., Edwards, R.L., Hoff, J., Gallup, C.D., Richards, D.A., Asmerom, Y., 2000. The half-lives of uranium-234 and Thorium-230. Chem. Geol. 169, 17–33.
Clark, D.H., 2003. Complex timing and patterns of glaciation in the American Cordillera during Termination I. XVI INQUA Congress Program with Abstracts. Paper 88-4, 231.
Clark, P.U., Bartlein, P.J., 1995. Correlation of late Pleistocene glaciation in the western United States with North Atlantic Heinrich events. Geology 23, 483–486.
Clark, D.H., Gillespie, A.R., 1997. Timing and significance of Late-Glacial and Holocene cirque glaciation in the Sierra Nevada, California. Quat. Int. 38/39, 21–38.
Clark, W.B., Lydon, P.A., 1962. Mines and Mineral Resources of Calaveras County, California. California Division of Mines and Geology, San Francisco.
Cole, K., 1983. Late Pleistocene vegetation of Kings Canyon, Sierra Nevada, California. Quat. Res. 19, 117–129.

Please cite this article as: Oster, J.L., et al., Late Pleistocene California droughts during deglaciation and Arctic warming, Earth Planet. Sci. Lett. (2009), doi:10.1016/j.epsl.2009.10.003

Cruz Jr., F.W., Burns, S.J., Karmann, I., Sharp, W.D., Vuille, M., Ferrari, J.A., 2006. A stalagmite record of changes in atmospheric circulation and soil processes in the Brazilian subtropics during the Late Pleistocene. Quat. Sci. Rev. 25, 2749–2761.

Dansgaard, W., 1964. Stable isotopes in precipitation. Telus 16, 436–468.

Dansgaard, W., Johnsen, S.J., Clausen, H.B., Dahl-Jensen, D., Gundestrup, N.S., Hammer, C.U., Hvidberg, C.S., Steffensen, J.P., Sveinbjörnsdottir, A.E., Jouzel, J., Bond, G., 1993. Evidence for general instability of past climate from a 250-year ice core record. Nature 364, 218–220.

Davis, O.K., 1999. Pollen analysis of Tulare Lake, California: Great Basin-like vegetation in Central California during the full-glacial and early Holocene. Rev. Palaeobot. Palynol. 107, 249–257.

deMenocal, P., Ortiz, J., Guilderson, T., Adkins, J., Sarnthein, M., Baker, L., Yarusinksy, M., 2000. Abrupt onset and termination of the African Humid Period: rapid responses to gradual insolation forcing. Quat. Sci. Rev. 19, 347–361.

Denniston, R.F., Asmerom, Y., Polyak, V., Dorale, J.A., Carpenter, S.J., Trodick, C., Hoye, B., González, L.A., 2007. Synchronous millennial-scale climatic changes in the Great Basin and the North Atlantic during the last interglacial. Geology 35, 619–622.

Dorale, J.A., Edwards, R.L., Ito, E., Gonzalez, L.A., 1998. Climate and vegetation history of the midcontinent from 75 to 25 ka: a speleothem record from Crevice Cave, Missouri, USA. Science 282, 1871–1874.

Edwards, R.L., Chen, J.H., Wasserburg, G.J., 1987. 238U–234U–230Th–232Th systematics and the precise measurement of time over the past 500, 000 years. Earth Planet. Sci. Lett. 81, 175–192.

Ellwood, B.B., Gose, W.A., 2006. Heinrich H1 and 8200 yr BP climate events recorded in Hall's Cave, Texas. Geology 34, 753–756.

Fairchild, I.J., Borsato, A.F., Frisia, S., Hawkesworth, C.J., Huang, Y., McDermott, F., Spiro, B., 2000. Controls on trace element (Sr–Mg) compositions of carbonate cave waters: implications for speleothem climatic records. Chemical Geology 166, 255–269.

Fleming, K., Johnston, P., Zwartz, D., Yokoyama, Y., Lambeck, K., Chappell, J., 1998. Refining the eustatic sea-level curve since the last glacial maximum using far- and intermediate-field sites. Earth Planet. Sci. Lett. 163, 327–342.

Frappier, A.B., Sahagian, D., Carpenter, S.J., González, L.A., Frappier, B.R., 2007. Stalagmite stable isotope record of recent tropical cyclone events. Geology 35, 111–114.

Frisia, S., Borsato, A., Fairchild, I.J., McDermott, F., 2000. Calcite fabrics, growth mechanisms, and environments of formation in speleothems from the Italian Alps and Southwestern Ireland. J. Sed. Res. 70, 1183–1196.

Genty, D., Blamart, D., Ouahdi, R., Gilmour, M., Baker, A., Jouzel, J., Van-Exter, S., 2003. Precise dating of Dansgaard-Oeschger climate oscillations in Western Europe from stalagmite data. Nature 421, 833–837.

Genty, D., Blamart, D., Ghaleb, B., Plagnes, V., Causse, Ch., Bakalowicz, M., Zouari, K., Chkir, N., Hellstrom, J., Wainer, K., Bourges, F., 2006. Timing and dynamics of the last deglaciation from European and North African $\delta^{13}C$ stalagmite profiles — comparison with Chinese and South Hemisphere stalagmites. Quat. Sci. Rev. 25, 2118–2142.

Gosse, J.C., Evenson, E.B., Klein, J., Lawn, B., Middleton, R., 1995. Precise cosmogenic Be-10 measurements in western North America — support for a global Younger Dryas cooling. Geology 23, 877–880.

Hellstrom, J., 2006. U–Th dating of speleothems with high initial ^{230}Th using stratigraphical constraint. Quat. Geochronol. 1, 289–295.

Hellstrom, J.C., McCulloch, M.T., 2000. Multi-proxy constraints on the climatic significance of trace element records from a New Zealand speleothem. Earth Planet. Sci. Lett. 179, 287–297.

Hemming, S.R., 2004. Heinrich events: massive late Pleistocene detritus layers of the North Atlantic and their global climate imprint. Rev. Geophys. 42, RG1005. doi:10.1029/2003RG000128.

Hendy, C.H., 1971. The isotopic geochemistry of speleothems — I. The calculation of the effects of different modes of formation on the isotopic composition of speleothems and their applicability as palaeoclimatic indicators. Geochim. Cosmochim. Acta 35, 801–824.

Hendy, I.L., Kennett, J.P., Roark, E.B., Ingram, B.L., 2002. Apparent synchroneity of submillennial scale climate events between Greenland and Santa Barbara Basin, California from 30–10 ka. Quat. Sci. Rev. 21, 1167–1184.

Howell, P., Pisias, N., Ballance, J., Baughman, J., Ochs, L., 2006. ARAND Time-Series Analysis Software. Brown University, Providence, R.I.

Kienast, M., Kienast, S.S., Calvert, S.E., Eglinton, T.I., Mollenhauer, G., Francois, R., Mix, A.C., 2006. Eastern Pacific cooling and Atlantic overturning circulation during the last deglaciation. Nature 443, 846–849.

Kim, S.-T., O'Neil, J.R., 1997. Equilibrium and nonequilibrium oxygen isotope effects in synthetic carbonates. Science 61, 3461–3475.

Kim, S.-J., Crowley, T.J., Erickson, D.J., Govindasamy, B., Duffy, P.B., Lee, B.Y., 2008. High-resolution climate simulation of the last glacial maximum. Clim. Dyn. 31, 1–6.

Kutzbach, J.E., Wright Jr., H.E., 1985. Simulation of the climate of 18,000 years BP. Results for the North America/North Atlantic/European sector and comparison with the geologic record of North America. Quat. Sci. Rev. 4, 147–187.

Labeyrie, L., 2000. Glacial climate instability. Science 290, 1905–1907.

Lea, D.W., Pak, D.K., Peterson, L.C., Hughen, K.A., 2003. Synchroneity of tropical and high-latitude Atlantic temperatures over the last glacial termination. Science 301, 1361–1364.

Lin, J.C., Broecker, W.S., Hemming, S.R., Hajdas, I., Anderson, R.F., Smith, G.I., Kelley, M., Bonani, G., 1998. A reassessment of U–Th and ^{14}C ages for late-glacial high-frequency hydrological events at Searles Lake, California. Quat. Res. 49, 11–23.

Lorens, R.B., 1981. Sr, Cd, Mn, and Co distribution coefficients in calcite as a function of calcite precipitation rate. Geochim. Cosmochim. Acta 45, 553–561.

Ludwig, K.R., 2003. Using Isoplot/Ex, Version 2.01: a geochronological toolkit for Microsoft Excel. Berkeley Geochronology Center Special Publication, vol. 1a. Berkeley Geochronology Center, Berkeley, California. 47 pp.

Ludwig, K.R., Wallace, A.R., Simmons, K.R., 1985. The Schwartzwalder uranium deposit, II: age of uranium mineralization and Pb-isotope constraints on genesis. Econ. Geol. 80, 1858–1871.

MacDonald, G.M., Moser, K.A., Bloom, A.M., Porinchu, D.F., Potito, A.P., Wolfe, B.B., Edwards, T.W.D., Petel, A., Orme, A.R., Orme, A.J., 2008. Evidence of temperature depression and hydrological variations in the eastern Sierra Nevada during the Younger Dryas stade. Quat. Res. 70, 131–140.

Machel, H.G., Cavell, P.A., Patey, K.S., 1996. Isotopic evidence for carbonate cementation and recrystallization, and for tectonic expulsion of fluids into the Western Canada Sedimentary Basin. Geol. Soc. Am. Bull. 108, 1108–1119.

Manabe, S., Stouffer, R.J., 1988. Two stable equilibria of a coupled ocean-atmosphere model. J. Climate 1, 841–866.

McDermott, F., 2004. Palaeo-climate reconstruction from stable isotope variation in speleothems: a review. Quat. Sci. Rev. 23, 901–918.

Meese, D.A., Gow, A.J., Alley, R.B., Zielinski, G.A., Grootes, P.M., Ram, M., Taylor, K.C., Mayewski, P.A., Bolzan, J.F., 1997. The Greenland ice sheet project 2 depth-age scale: methods and results. J. Geophys. Res. 102, 26,411–26,423.

Mensing, S.A., 2001. Late-Glacial and early Holocene vegetation and climate change near Owens Lake, Eastern California. Quat. Res. 55, 57–65.

Mickler, P.J., Banner, J.L., Stern, L., Asmerom, Y., Edwards, R.L., Ito, E., 2004. Stable isotope variations in modern tropical speleothems: evaluating equilibrium vs. kinetic isotope effects. Geochim. Cosmochim. Acta 68, 4381–4393.

Mickler, P.J., Stern, L.A., Banner, J.L., 2006. Large kinetic isotope effects in modern speleothems. Geol. Soc. Am. Bull. 118, 65–81.

Mikolajewicz, U., Crowley, T.J., Schiller, A., Voss, R., 1997. Modelling teleconnections between the North Atlantic and North Pacific during the Younger Dryas. Nature 387, 384–387.

Montañez, I.P., Osleger, D.A., Banner, J.L., Mack, L., Musgrove, M.L., 2000. Evolution of the Sr and C isotope composition of Cambrian oceans. GSA Today 10, 1–5.

Musgrove, M., Banner, J.L., Mack, L.E., Combs, D.M., James, E.W., Cheng, H., Edwards, R.L., 2001. Geochronology of late Pleistocene to Holocene speleothems from central Texas: Implications for regional paleoclimate. Geol. Soc. Am. Bull. 113, 113–1543.

Oviatt, C.G., Miller, D.M., McGeehin, J.P., Zachary, C., Mahan, S., 2005. The Younger Dryas phase of the Great Salt Lake, Utah, USA. Palaeogeography, Palaeoclimatology, Palaeoecology 219, 263–284.

Owen, L.A., Finkel, R.C., Minnich, R.A., Perez, A.E., 2003. Extreme southwestern margin of late Quaternary glaciation in North America: timing and controls. Geology 31, 729–732.

Peterson, L.C., Haug, G.H., Hughen, K.A., Röhl, U., 2000. Rapid changes in the hydrologic cycle of the tropical Altantic during the Last Glacial. Science 290, 1947–1951.

Phillips, L.C., Zreda, M., Plummer, M.A., Elmore, D., Clark, D.H., 2009. Glacial geology and chronology of Bishop Creek and vicinity, eastern Sierra Nevada, California. Geol. Soc. Am. Bull. 121, 1013–1033.

Polyak, V.J., Rasmussen, J.B.T., Asmerom, Y., 2004. Prolonged wet period in the southwestern United States through the Younger Dryas. Geology 32, 5–8.

Quade, J., Cerling, T.E., Bowman, J.R., 1989. Systematic variations in the carbon and oxygen isotopic composition of pedogenic carbonate along elevation transects in the southern Great Basin, United States. Geol. Soc. Am. Bull. 101, 464–475.

Rozanski, K., Araguas-Araguas, L., Gonfiantini, R., 1993. Isotopic patterns in modern global precipitation. In: Swart, P.K., et al., (Eds.), Climate change in continental isotope records: American Geophysical Union Monographs. p. 1–36.

Seager, R., Ting, M., Held, I., Kushnir, Y., Lu, J., Vecchi, G., Huang, H.-P., Harnik, N., Leetmaa, A., Lau, N.-C., Li, C., Velez, J., Naik, N., 2007. Model projections of an imminent transition to a more arid climate in southwestern North America. Science 316, 1181–1184.

Sewall, J.O., 2005. Precipitation shifts over Western North America as a result of declining Arctic sea ice cover: the coupled system response. Earth Interact. 9 (26).

Sewall, J.O., Sloan, L.C., 2004. Disappearing Arctic sea ice reduces available water in the American west. Geophys. Res. Lett. 31. doi:10.1029/2003GL019133.

Short, H.W., 1975. The geology of Moaning Cave, Calaveras County, California. Calif. Geol. 28, 195–201.

Stuiver, M., Grootes, P.M., 2000. GISP2 oxygen isotope ratios. Quat. Res. 53, 277–284.

Thompson, R.S., Whitlock, C., Bartlein, P.J., Harrison, S.P., Spaulding, W.G., 1993. Climatic changes in the western United States since 18,000 yr B.P. In: WrightJr. Jr., H.E., Kutzbach, J.E., WebbIII III, T., Ruddiman, W.F., Street-Perrott, F.A., Bartlein, P.J. (Eds.), Global Climates since the Last Glacial Maximum. University of Minnesota Press, Minneapolis. 569 pp.

Vacco, D.A., Clark, P.U., Mix, A.C., Cheng, H., Edwards, R.L., 2005. A speleothem record of Younger Dryas cooling, Klamath Mountains, Oregon, USA. Quat. Res. 64, 249–256.

Vaks, A., Bar-Matthews, M., Ayalon, A., Schilman, B., Gilmour, M., Hawkesworth, C.J., Frumkin, A., Kaufman, A., Matthews, A., 2003. Paleoclimate reconstruction based on the timing of speleothem growth and oxygen and carbon isotope composition in a cave located in the rainshadow in Israel. Quat. Res. 59, 182–193.

Vellinga, M., Wood, R.A., 2002. Global climatic impacts of a collapse of the Atlantic thermohaline circulation. Clim. Change 54, 251–267.

von Grafenstein, U., Erlenkeuser, H., Brauer, A., Jouzel, J., Johnsen, S.J., 1999. A mid-European decadal isotope-climate record from 15,500 to 5000 years B.P. Science 284, 1654–1657.

Wang, Y.J., Cheng, H., Edwards, R.L., An, Z.S., Wu, J.Y., Shen, C.-C., Dorale, J.A., 2001. A high-resolution absolute-dated Late Pleistocene monsoon record from Hulu Cave, China. Science 294, 2345–2348.

Wang, X., Auler, A.S., Edwards, R.L., Cheng, H., Cristalli, P.S., Smart, P.L., Richards, D.A., Shen, C.-C., 2004. Wet periods in northeastern Brazil over the past 210 kyr linked to distant climate anomalies. Nature 432, 740–743.

Wang, Y., Cheng, H., Edwards, R.L., He, Y., Kong, X., An, Z., Wu, J., Kelly, M.J., Dykoski, C.A., Li, X., 2005. The Holocene Asian Monsoon: links to solar changes and North Atlantic climate. Science 308, 854–857.

Winograd, I.J., Landwehr, J.M., Coplen, T.B., Sharp, W.D., Riggs, A.C., Ludwig, K.R., Kolesar, P.T., 2006. Devils Hole, Nevada, $\delta^{18}O$ record extended to the mid-Holocene. Quat. Res. 66, 202–212.

Yuan, D.X., Cheng, H., Edwards, R.L., Dykoski, C.A., Kelly, M.J., Zhang, M.L., Qing, J.M., Lin, Y.S., Wang, Y.J., Wu, J.Y., Dorale, J.A., An, Z.S., Cai, Y.J., 2004. Timing, duration, and transitions of the Last Interglacial Asian Monsoon. Science 304, 575–578.

Please cite this article as: Oster, J.L., et al., Late Pleistocene California droughts during deglaciation and Arctic warming, Earth Planet. Sci. Lett. (2009), doi:10.1016/j.epsl.2009.10.003